

# Evanescent fields & Bottle resonators

Quantenpraktikum



Prof. Dr. Arno Rauschenbeutel  
Technische Universität Wien

# Contents

<b>1</b>	<b>Microresonators: Basic Principles</b>	<b>4</b>
1.1	Fabry-Pérot Microresonators . . . . .	4
1.2	Whispering-Gallery Mode Resonators . . . . .	6
1.2.1	Total Internal Reflection & Evanescent Waves . . . . .	7
1.2.2	Whispering Gallery Modes in a Bottle Resonator . . . . .	9
1.2.3	Optical Fibers . . . . .	9
<b>2</b>	<b>Coupling between Bottle Modes and Ultra-Thin Optical Fibers</b>	<b>10</b>
2.1	Modeling the Ultra-Thin Fiber – Resonator Coupling . . . . .	10
<b>3</b>	<b>Experimental Setup</b>	<b>12</b>
3.1	Mechanical Components . . . . .	12
3.2	Optical Components . . . . .	13
<b>4</b>	<b>Laser Safety</b>	<b>16</b>
4.1	Handling Instructions . . . . .	16
<b>5</b>	<b>Experimental Procedure</b>	<b>17</b>
5.1	Startup . . . . .	17
5.2	Excitation of a WGM . . . . .	18
5.3	Evanescent Coupling with an air gap . . . . .	21
5.4	Evanescent Coupling and Resonator Properties as a function of Resonator–Fiber Gap . . . . .	22
<b>6</b>	<b>Analysis</b>	<b>24</b>
6.1	Resonator Properties . . . . .	24
6.2	Losses introduced by the Ultra-Thin Coupling Fiber . . . . .	25
<b>7</b>	<b>Writing the Report</b>	<b>27</b>
<b>8</b>	<b>Optional Exercises</b>	<b>29</b>

<b>A Appendices</b>	<b>30</b>
A.1 Emission of green fluorescence from bottle modes . . . . .	30

## Abstract

In this experiment you will learn about a state-of-the-art resonator designed from optical glass fibers. The experiment will teach you about the theory and practice of *evanescent-waves*, *sub-micron-diameter fibers* capable of lossless guiding of light, and how to characterize a resonator based on the principles of *whispering-gallery modes* (WGM). Taken together, these three aspects of the experiment will show you how WGM-based resonators exhibit fundamentally different characteristics to the more traditional Fabry-Pérot (FP) resonator that you've learned about in your studies to date.

§§§

## 1 Microresonators: Basic Principles

At the heart of the experiment is a so-called "whispering gallery mode resonator". An important property of this resonator is the quality factor, which, unlike for the FP resonator, can be easily controlled to give the desired performance. In the case of WGM resonators, this quantity, which is a measure of photon storage time, is governed by the strength of overlapping evanescent waves. By manipulating the overlap of two evanescent waves, you will demonstrate the highly efficient and lossless coupling of light to a WGM resonator. In particular, light can be coupled with >99 % efficiency into the resonator once the overlap is optimal. (Note: For FP resonators with high quality factor, such a feat is actually not possible due to absorption and scattering losses of the mirrors).

The setup is largely fiber-based and driven manually using stepper motors and a piezoelectric actuator. The center-pieces of the setup are the *bottle resonator* (a type of WGM resonator developed at the Atominstitut) and the sub-micron-diameter fiber (which, for clarity, we will instead call the *coupling fiber* in the following text). One of the main tasks of the experiment is the alignment of the coupling fiber and the bottle resonator. To understand the physics, we first consider the common Fabry-Pérot resonator since many of its properties can be directly applied to the WGM resonator.

### 1.1 Fabry-Pérot Microresonators

The Fabry-Pérot resonator can be seen as the prototype resonator. A typical Fabry-Pérot microresonator (also referred to as a microcavity in other literature) consists of two millimeter-sized mirrors with a separation of  $L = 10 - 160 \mu\text{m}$ . Repeated reflections of the light from the reflective mirror means that the light field of the cavity can be described by a Gaussian standing wave profile, as shown in Fig. 1. A standing wave is created when the in-coupled light obeys the condition

$$l = i \frac{\lambda_0}{2n}, \quad \text{with } i = 1, 2, 3, \dots \quad (1)$$

where  $l$  is the length of the resonator and is an integer number of half-wavelengths, the vacuum wavelength is  $\lambda_0$  and  $n$  is the refractive index of the medium.

Consider now the transmitted light (in/out-coupling is done through the partially reflective mirror), the maximal transmission occurs at the resonance frequencies. At these particular

frequencies there is constructive interference between the incoming light field and the intracavity field:

$$\nu_i = i \frac{c}{2nl}, \quad \text{with } i = 1, 2, 3, \dots \quad (2)$$

where  $c$  is the speed of light in vacuum. In the ideal case of a resonator with no losses, the transmission is only at discrete values of  $\nu_i$ . In a real resonator, losses give rise to a Lorentz-shaped transmission profile.

The transmitted power  $P_{\text{tr,FP}}$ , which is proportional to the intracavity intensity, is given by an Airy function

$$P_{\text{tr,FP}} = \frac{4t^2(1-a)}{(2t+a)^2} \frac{P_{\text{in}}}{1 + F_A \sin^2(\delta/2)}, \quad (3)$$

with the generalized finesse coefficient  $F_A = 4r\sqrt{1-a}/(1-r\sqrt{1-a})^2$ . Figure 2 (a) shows  $P_{\text{tr,FP}}$  as a function of the optical frequency of the input wave.

The mirrors of high- $Q$  microresonators usually consist of multi-layer dielectric coatings which have a low transmission  $t$  in the ppm (*parts per million*) range in order to enable a maximum storage time of the light. Losses result from leakage of photons from the cavity due to the finite reflectivity  $r$  of the coatings as well as from absorption and scattering losses  $a$  (the coefficients  $t$ ,  $r$  and  $a$  describe the change in intensity due to transmission, reflection and absorption by the cavity's mirrors for one round trip). Therefore, in the absence of a driving light field, the intracavity energy  $W$  decays exponentially with a time constant  $\tau$ . The first loss mechanism enables coupling of propagating light fields to the cavity mode and is therefore inevitable. The latter are referred to as intrinsic losses resulting from imperfections in the resonator material and fabrication.

The temporal confinement can be quantitatively described by the storage time  $\tau$  in units of the optical period  $T = \nu_0^{-1}$ , with the optical resonance frequency  $\nu_0$ . It is convenient to use the “so-called” quality factor  $Q$  which is defined as

$$Q = 2\pi \frac{\tau}{T}. \quad (4)$$

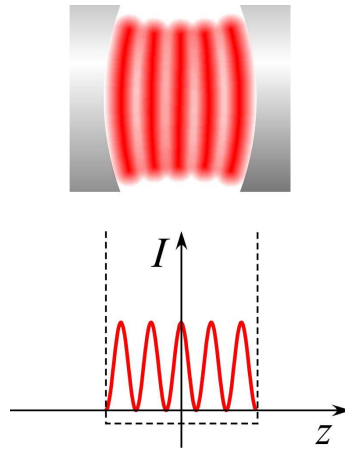


Figure 1: Basic principle of a Fabry-Pérot resonator consisting of two highly reflecting mirrors. The cavity mode is a Gaussian beam exhibiting a standing wave structure.

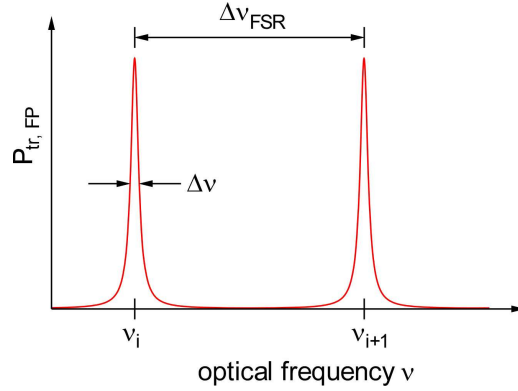


Figure 2: Mode spectrum of the transmission of a Fabry-Pérot resonator. The power transmitted through the cavity  $P_{tr}$  as a function of the optical frequency of the input light field is given by an Airy function. The signal transmitted through the cavity,  $P_{tr,FP}$ , is proportional to the intracavity intensity. The individual peaks/dips of FWHM  $\Delta\nu$ , corresponding to the modes of the resonator, are separated by the free spectral range  $\Delta\nu_{FSR}$ .

Using the angular resonance frequency  $\omega_0 = 2\pi\nu_0$ , the quality factor is written as  $Q = \omega_0\tau$ .

Since in Fabry Pérot resonators, unlike as in WGM resonators, the losses almost exclusively occur at each reflection, it is convenient to characterize these devices by the cavity's finesse  $\mathcal{F}$ , which is related to the number of round trips  $N$  of the light within the storage time  $\tau$  by

$$\mathcal{F} = 2\pi N . \quad (5)$$

The light field in the resonator is enhanced by a factor proportional to  $N$ , giving rise to huge power densities in microresonators, e.g. hundreds of  $\text{MW}/\text{cm}^2$  for 1 mW in-coupled power. The frequency spacing between adjacent modes of orders  $i$  and  $i + 1$ , is called free spectral range  $\Delta\nu_{FSR} = \nu_{i+1} - \nu_i$ . The FWHM of the resonances is denoted by  $\Delta\nu$ . It can be shown that the finesse is given by the ratio of both quantities

$$\mathcal{F} = \frac{\Delta\nu_{FSR}}{\Delta\nu} . \quad (6)$$

As a consequence, the quality factor can be expressed as the ratio of linewidth to optical frequency of the resonance  $\nu_0$

$$Q = \frac{\nu_0}{\Delta\nu} . \quad (7)$$

The transmission through the cavity, determined by the intrinsic losses rate  $a$ , on resonance reaches a maximum value of  $T = P_{tr,FP}/P_{in} = 4t^2(1-a)/(2t+a)^2 \approx t^2/(t+a)^2$ .

## 1.2 Whispering-Gallery Mode Resonators

Another, more elegant type of resonator are WGM resonators, so-named after acoustic modes St. Paul's Cathedral, as explained in Fig. 4. Light confinement in WGM resonators is based on total internal reflection. We can use *frustrated* total internal reflection to efficiently couple a propagating light field to WGMs. Therefore these phenomena will be briefly reviewed in some detail. For further reading, see [Vah03].

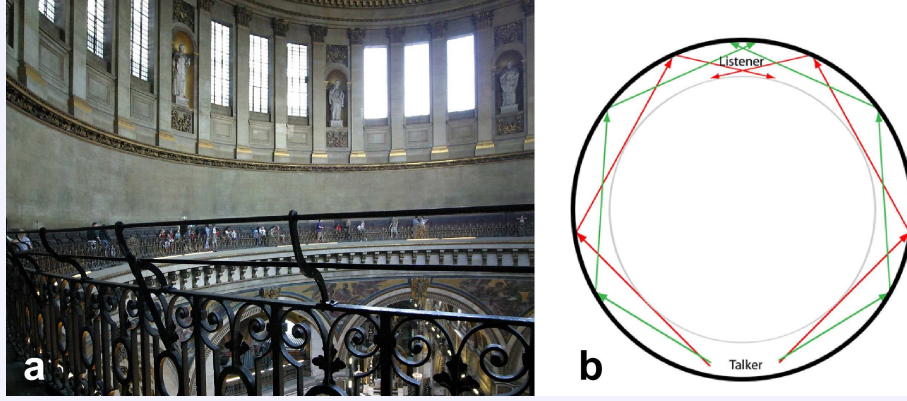


Figure 4: **WGMs in St. Paul's Cathedral, London**

In 1910, Lord Raleigh explained the well known, but unusual, phenomenon observed in the dome of St. Paul's Cathedral (left) where a person's whisper near the wall at any point is audible to a listener near the wall at any other point around the gallery. The gallery is 31 m in diameter! And hence the origin of the term *whispering gallery modes* to describe acoustic and optical modes.

### 1.2.1 Total Internal Reflection & Evanescent Waves

The refraction of an electromagnetic wave, propagating in a medium of refractive index  $n_1$  at an interface with another medium of refractive index  $n_2$  is described by Snell's law [Hec89]

$$n_1 \sin(\theta_1) = n_2 \sin(\theta_2) , \quad (8)$$

where  $\theta_1, \theta_2$  are the angles between the wave vectors  $\vec{k}_1$  and  $\vec{k}_2$  of the incident and refracted light fields and the surface's normal vector, respectively, as illustrated in Fig. 5 (a). At an interface between an optically dense medium and an optically thinner medium, i.e., for  $n_2 < n_1$ , a reflected wave only exists for angles  $\theta_1$  smaller than the critical angle  $\theta_c = \sin^{-1}(n_2/n_1)$ . Otherwise, the incident wave is totally reflected from the interface, as shown in Fig. 5 (b) At a glass-air interface with  $\Delta n \approx 0.5$  the critical angle is  $42^\circ$ . In the following, the electromagnetic field in the optically thinner medium in the case of total internal reflection will be examined, following the analysis in [Mes04, Hec89]. For simplicity, the electric field in the optically thinner medium is treated as a scalar field of the form

$$E_2 = E_{02} \exp\left(i\left(\vec{k}_2 \cdot \vec{r} - \omega t\right)\right) . \quad (9)$$

The wave vector  $\vec{k}_2$  with an absolute value of  $|\vec{k}_2| = n_2 2\pi / \lambda_0$  can be split in a component  $k_x$  that describes the propagation along the interface and a component  $k_y$  describing the propagation normal to the interface. Using Snell's law one finds a relation for  $k_y = k_2 \cos(\theta_2)$

$$k_y = k_2 \left(1 - \frac{n_1^2 \sin^2(\theta_1)}{n_2^2}\right)^{1/2} . \quad (10)$$

If  $\sin(\theta_1) > n_2/n_1$ ,

$$k_y = ik_2 \left(\frac{n_1^2 \sin^2(\theta_1)}{n_2^2} - 1\right)^{1/2} = i\beta \quad (11)$$

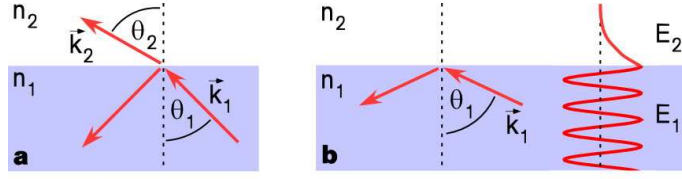


Figure 5: (a) Reflection and refraction at an interface between two media with refractive indices  $n_1$  and  $n_2$ . The wave vector of the incident wave and the refracted wave are denoted by  $\vec{k}_1$  and  $\vec{k}_2$ , respectively. The relation between their angles with the normal vector of the interface,  $\theta_1$  and  $\theta_2$ , is described by Snell's law. (b) For  $n_2 < n_1$  and angles larger than the critical angle  $\theta_c$  the light field is completely reflected by the interface. A detailed analysis shows that the electromagnetic field decays exponentially beyond the interface. The penetration depth of this evanescent field into the other medium is typically on the length-scale of the wavelength.

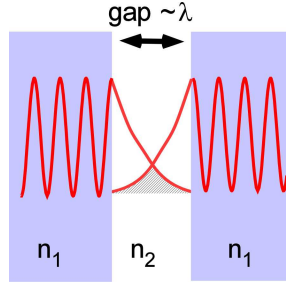


Figure 6: Frustrated total internal reflection between two media, e.g., between a glass coupling fiber and a glass resonator. Light in one medium can couple to a second medium because the evanescent fields overlap, despite the media not having direct physical contact.

becomes **complex**, while  $k_x = (n_1 k_2 / n_2) \sin(\theta_1)$  is **real**. The electric field strength in the optically thinner medium is given by

$$E_2 = E_{02} \exp(-\beta y) \exp i(k_x x - \omega t) . \quad (12)$$

This so-called “evanescent field” exponentially decays with increasing distance  $y$  from the interface. Its decay length

$$\frac{1}{\beta} = \frac{\lambda_0}{2\pi \sqrt{n_1^2 \sin^2(\theta_1) - n_2^2}} \quad (13)$$

is typically on the order of the wavelength.

A propagating light field in one medium can be coupled into a second medium if they are both placed close enough so that the evanescent fields overlap, as shown in Fig. 6. This phenomenon, called “frustrated total internal reflection”, is used to couple light from an optical fiber into a resonator and visa versa. The amount of transmitted light is controlled by varying the width of the gap. This is described in Sec. 2.



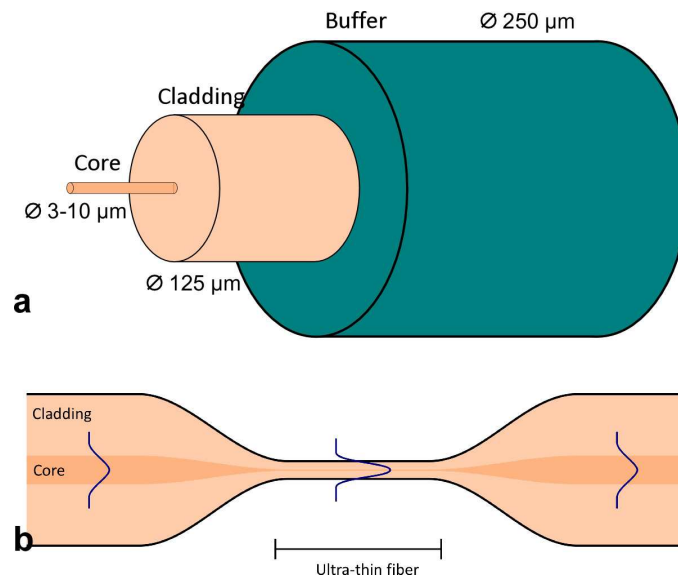


Figure 7: (a) A cross-section of an optical fiber. (b) Using the fiber in (a), it is possible to make an ultra-thin fiber with a diameter of 500 nm. In this part of the fiber, a fraction of the light field is outside the fiber in the evanescent field.

### 1.2.2 Whispering Gallery Modes in a Bottle Resonator

While there are a few different resonator designs for creating WGMs (for example, see [Vah03]), perhaps the most exotic design is the *bottle resonator*. In the same way that sound propagates around the circular dome in St. Paul's Cathedral (Fig. 4), light also propagates around in a circle in a bottle resonator made from glass.

Comparing the Fabry-Pérot resonator in Fig. 1 and the bottle resonator in Fig. 8 (a,b), there are a number of obvious differences; the bottle resonator has a quasi-cylindrical geometry, the light path is circular and can have multiple rings of light. A mode with two rings of light is shown in Fig. 8 (b), and other modes can have anywhere up to several hundred rings. A mode with two rings will have a different resonance frequency to a mode with three rings and so on. We note that many of the properties of the Fabry-Pérot resonator are also valid for the bottle resonator, such as, the resonance condition (Eq. 1, with  $l$  being the circumference), mode frequencies (Eq. 2),  $Q$ -factor and finesse (Eqs. 4, 5, 6, 7). For further reading, see the articles in the appendix.

### 1.2.3 Optical Fibers

Optical fibers are widely used in everyday life to do some basic, but very important, tasks. For example, fibers guide optical data with gigahertz transfer rates in order to provide high speed internet, amongst other things. Light is guided in the core of the fiber in Fig. 7 (a) because it is trapped by total internal reflection ( $n_{\text{core}} > n_{\text{clad}}$ ). In this experiment, we use a specially made optical fiber with an ultra-thin section of only 500 nm in diameter as shown in Fig. 7 (b). For further reading, see the articles in the appendix.

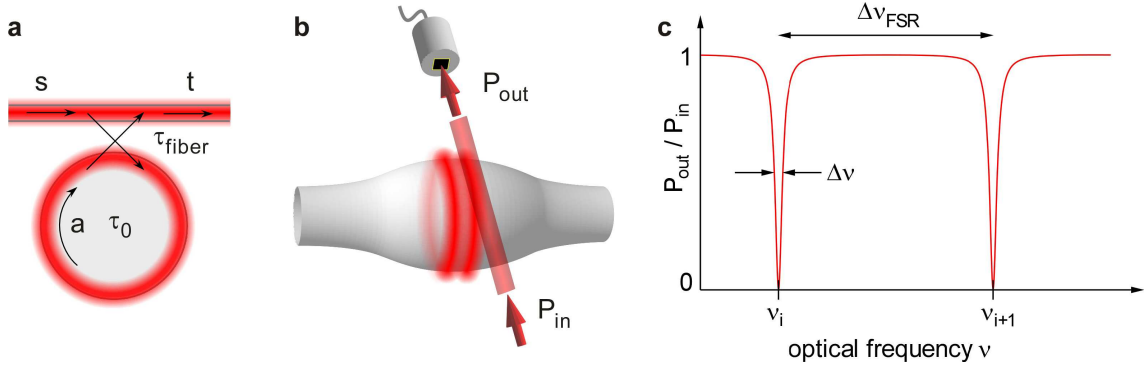


Figure 8: (a) The coupling point between the coupling fiber and the bottle microresonator can be described by a simple model. The “mode amplitude” of the bottle microresonator is denoted by  $a$ , whereas  $s$  and  $t$  are the “input field amplitude” and the “output field amplitude” of the waveguide. Characteristic time constants  $\tau_{\text{fiber}}$  and  $\tau_0$  describe the transfer of optical energy between both fibers and the intrinsic resonator energy loss. (b) In the experiment, the power transmitted through the coupling fiber  $P^{\text{out}} = |t|^2$  is measured for a given input power  $P_{\text{in}} = |s|^2$  and varying width  $x$  of the coupling gap. (c) The transmission spectrum of a WGM resonator has an inverted shape compared to the transmission of a Fabry-Pérot resonator (Fig. 2).

## 2 Coupling between Bottle Modes and Ultra-Thin Optical Fibers

As mentioned earlier, light can be coupled into a WGM resonator by overlapping it with the evanescent field of an ultra-thin coupling fiber. In this section, we give a general model [Hau84] describing the transfer of optical energy between an input light field in a coupling fiber and a WGM resonator.

The coupling between the bottle mode and the coupling fiber can be tuned by adjusting the width  $x$  of the coupling gap. The influence of the width of this gap on the coupling characteristics and the quality factor of the bottle mode is a main focus of this experiment and is discussed in the following. It is shown below that at the so-called “critical coupling point” a complete transfer of the optical power to the resonator mode is possible. It is also possible to determine if the ultra-thin fiber coupler causes scattering losses.

### 2.1 Modeling the Ultra-Thin Fiber – Resonator Coupling

In [Hau84] a general formalism that describes the coupling of a resonator to an external light field is presented. Using this model the coupling point between a bottle mode and the coupling fiber is described using the parameters schematically indicated in Fig. 8 (a,b).

It is assumed that a bottle mode with resonance frequency  $\nu_0 = \omega_0/2\pi$  is excited by a light field of frequency  $\omega$  propagating in the coupling fiber. The optical energy  $W$  stored in the mode of the bottle microresonator is obtained from its mode amplitude  $a$  via  $W = |a|^2 = aa^*$ . The transfer of optical energy between the mode of the coupling fiber and the bottle mode is described by a characteristic time constant  $\tau_{\text{fiber}}$ . This parameter exhibits a strong dependence on the width  $x$  of the coupling gap because it is determined by the spatial overlap between

the evanescent fields of both structures. The loss of energy through intrinsic resonator losses like absorption or scattering from glass and surface roughness is described by  $\tau_0$ . The optical power sent through the coupling fiber is given by  $P_{\text{in}} = |s|^2 = s s^*$  using the input field amplitude  $s$ . From the output field amplitude  $t$ , the power transmitted through the coupling fiber is obtained from  $P_{\text{out}} = |t|^2 = t t^*$ . The coupling fiber transmission is defined as  $P_{\text{out}}/P_{\text{in}} = |t/s|^2$ . According to [Hau84], the system is then described by the following differential equation

$$\frac{d}{dt}a = i(\omega_0 - \omega)a - \frac{1}{2}(\tau_0^{-1} + \tau_{\text{fiber}}^{-1})a + \tau_{\text{fiber}}^{-1/2}s. \quad (14)$$

Note that  $|s|^2$  represents the running wave in the fiber with an optical power in units J/s whereas  $|a|^2$  is the optical energy stored in the resonator given in J. The first term describes the fact that power buildup in the resonator is only possible at a discrete frequency  $\omega_0$ , at which the resonance condition is fulfilled. The second term describes the decay of the mode amplitude due to intrinsic resonator losses and the presence of the coupling fiber. The third term describes the coupling to the driving light field incident through the coupling fiber. The exact expression describing how  $\tau_{\text{fiber}}$  couples  $a$  and  $s$  in the last term of the above equation is derived in [Hau84] by time reversal symmetry. Next, the equation is solved in the absence of a driving light field

$$\frac{d}{dt}W = a^* \frac{d}{dt}a + a \frac{d}{dt}a^* = -(\tau_0^{-1} + \tau_{\text{fiber}}^{-1})W. \quad (15)$$

In this case, the energy stored in the resonator mode decays exponentially due to intrinsic losses and back-coupling to the coupling fiber

$$W = W_0 \exp(-t(\tau_0^{-1} + \tau_{\text{fiber}}^{-1})) = W_0 \exp(-t/\tau_{\text{load}}). \quad (16)$$

The overall time constant of the energy decay is then given by  $\tau_{\text{load}}^{-1} = \tau_{\text{fiber}}^{-1} + \tau_0^{-1}$  and the loaded quality factor in the presence of the coupling fiber is thus given by  $Q_{\text{load}} = \omega_0 \tau_{\text{load}}$ . It is possible to separate the different physical effects that contribute to the loaded quality factor

$$Q_{\text{load}}^{-1} = (\omega \tau_0)^{-1} + (\omega \tau_{\text{fiber}})^{-1} = Q_0^{-1} + Q_{\text{fiber}}^{-1} \quad (17)$$

and thus to define an intrinsic quality factor  $Q_0$  which only includes the intrinsic resonator losses. The loss mechanism with the smallest time constant will dominate  $Q_{\text{load}}$ .

As a function of the frequency of the driving field, the resonance appears as a Lorentzian-shaped dip in the coupling fiber transmission (see Fig.8 (c)). Its FWHM (full width at half maximum) is  $\Delta\omega = \tau_{\text{fiber}}^{-1} + \tau_0^{-1} = \tau_{\text{load}}^{-1}$ , corresponding to a spectral linewidth of  $\Delta\nu = (2\pi \cdot \tau_{\text{load}})^{-1}$ . This means that the loaded quality factor can also be inferred from the FWHM linewidth of the resonance in the signal transmitted through the coupling fiber

$$Q_{\text{load}} = \omega_0 \cdot \tau_{\text{load}} = \frac{\nu_0}{\Delta\nu}. \quad (18)$$

Progressively decreasing the gap between the coupling fiber and the resonator reduces  $\tau_{\text{fiber}}$ . This leads to a decrease in  $Q_{\text{load}}$ , which is apparent in a broadening of the Lorentzian-shaped resonance dip. Moreover, it is common to classify different coupling regimes dependent on the ratio  $\tau_0/\tau_{\text{fiber}}$ .

1. **Under-coupled regime:**  $\tau_{\text{fiber}} > \tau_0$ . For a large coupling gap  $x$ , for which  $\tau_{\text{fiber}} \gg \tau_0$ ,  $T_{\text{res}}$  is close to unity and increases with  $x$ . Only a fraction of the power incident through the coupling fiber is transferred to the resonator, where it is dissipated.

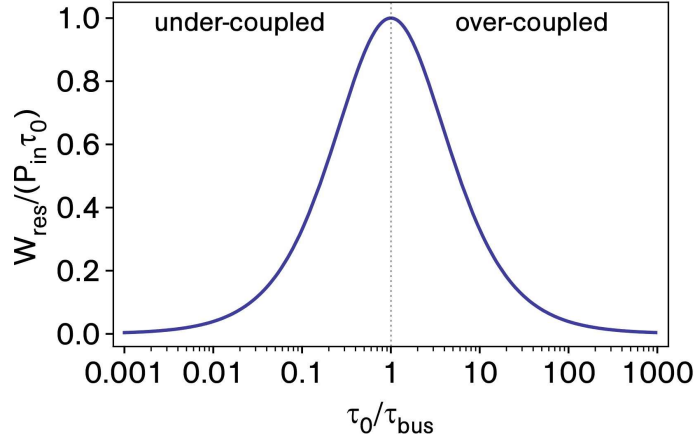


Figure 9: Energy stored inside a bottle mode on resonance  $W_{\text{res}} = |a(\omega = \omega_0)|^2$  as a function of  $\tau_0/\tau_{\text{fiber}}$ . A maximum value of  $P_{\text{in}} \cdot \tau_0$  is reached at critical coupling. This value corresponds to the power incident through the coupling fiber integrated during the intrinsic energy storage time  $\tau_0$ .

2. **Critical coupling:**  $\tau_{\text{fiber}} = \tau_0$ . For one particular gap distance the coupling time constant matches that of the intrinsic losses and the power incident through the coupling fiber is completely dissipated in the resonator. The light-field leaking from the resonator couples back into the waveguide and has an amplitude equal to the waveguide field transmitted past the resonator but has a phase shift of  $\pi$ . The almost zero transmission can thus be understood as destructive interference of both fields with equal amplitude. The corresponding quality factor is given by

$$Q_{\text{crit}} = \frac{\omega_0 \tau_0}{2} = \frac{Q_0}{2}. \quad (19)$$

3. **Over-coupled regime:**  $\tau_{\text{fiber}} < \tau_0$ . A further reduction of the gap results in a recovery of the relative transmission to 1. In this regime, the amplitude of the cavity leakage field is larger than that of the transmitted waveguide field.

It is possible to calculate the energy stored inside the bottle mode on resonance  $W_{\text{res}} = |a(\omega = \omega_0)|^2$  as a function of  $\tau_0/\tau_{\text{fiber}}$ . The result is plotted in Fig. 9.

### 3 Experimental Setup

In the experiment we want to experimentally analyze the properties of a bottle GM resonator together with an ultra-thin coupling fiber. For this purpose, we next turn our attention to the mechanical and optical components of the experimental setup used to excite bottle modes.

#### 3.1 Mechanical Components

**Fiber holder:** The resonator fiber and the coupling fiber are attached to specialized holders. A schematic of the bottle fiber holder design is shown in Fig. 10.

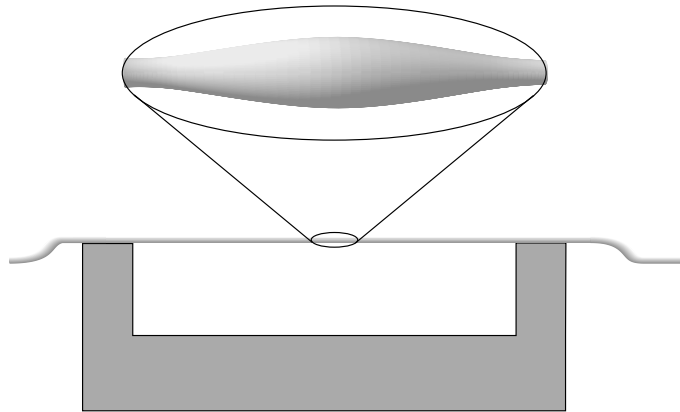


Figure 10: Schematic of the fiber holder design used to hold the resonator fiber and coupling fiber. The zoomed section shows a bottle resonator. A second holder is used for the coupling fiber.

**Positioning of the coupling fiber:** A positioning system is used to move the coupling fiber into place at a particular bottle mode in close proximity to the resonator surface. The coupling fiber is mounted horizontally while the resonator is mounted vertically. The positioning system consists of three orthogonally oriented translation stages (Physik Instrumente GmbH). A photograph of the positioning system is shown in Fig. 11.

- **Control of the coupling gap:** The width of the coupling gap,  $x$ , between the coupling fiber and the resonator is in the range of the decay length of the evanescent fields of both structures, i.e., a few hundred nanometers, and is controlled with a resolution of 10 nm using a piezo-electric actuator (Physik Instrumente, P-854.00). A voltage of 0 – 60 V corresponds to a travel range of 15  $\mu\text{m}$ . Since the coupling has been pre-aligned by the instructor, the micrometer screw is not normally used.
- **Positioning along the resonator axis:** For coupling to different axial bottle modes the position of the coupling fiber can be scanned along the resonator axis via a micrometer screw with a resolution of 1  $\mu\text{m}$ . However, since the coupling has been pre-aligned by the instructor, it is not necessary to make this adjustment.

**Microscope:** An optical microscope and CMOS camera are used to image the bottle resonator modes. Green fluorescing bottle modes are clearly visible when excited with light from the coupling fiber. The microscope objective (Mitutoyo, M Plan APO 10 $\times$ ) has a working distance of 33.5 mm. It offers a resolution of 1  $\mu\text{m}$  and its depth of focus is 3.5  $\mu\text{m}$ . Using a lens tube the objective is connected to a color CMOS camera with a low pass filter at 650 nm (Thorlabs, DCC1645C). The extinction of the filter at 850 nm wavelength is, however, limited.

### 3.2 Optical Components

**DFB Laser at 850 nm:** The spatial and spectral properties of bottle modes are investigated using a distributed feedback (DFB) diode laser operating at a wavelength of around 850 nm

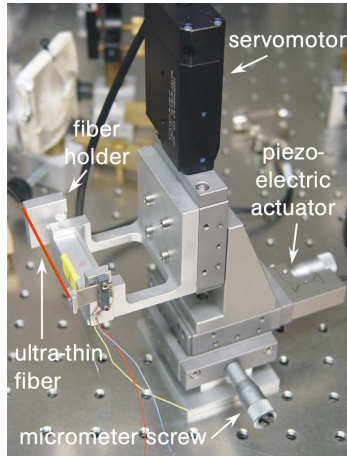


Figure 11: Mechanical system used for positioning an ultra-thin optical fiber (indicated by the red line on the left). Three orthogonally oriented stages driven by a piezo-electric actuator, a servomotor and a micrometer screw, respectively, are used to place the coupling fiber at a mode of the bottle microresonator.

with a short-term ( $< 5 \mu\text{s}$ ) linewidth of 400 kHz (Toptica Photonics, DL 100 DFB 1028). The frequency of the laser light  $\nu$  can be tuned over a maximum of 1.1 THz by modulation of the laser diode temperature, while fine tuning over a range of 20 GHz is achieved by changing the input current. A schematic of the optical setup is shown in Fig. 12.

The polarization of the probe light at the fiber waist is matched to the polarization of the bottle mode using a polarization controller consisting of quarter- and half-wave plates. A photodiode monitors the power transmitted through the fiber,  $P_{\text{out}}$ . The photodiode signal is recorded using a digital oscilloscope (GW INSTEK, GDS-2062), which is triggered by the wavelength scanner module of the laser controller. In order to monitor the laser frequency  $\nu$  during a measurement, several percent of the probe light power is split off using a half-wave plate and a polarizing beam splitter cube. This light is then sent through a reference Fabry-Pérot cavity. This cavity consists of a 1 m length of optical fiber with a mirror coating on each end. A photodiode monitors the transmitted power of the cavity. The cavity length of 1 m corresponds to a mode spacing of 100 MHz, which thus provides a frequency scale that allows one to measure the linewidth of bottle modes. A picture of the setup is shown in Fig. 13.

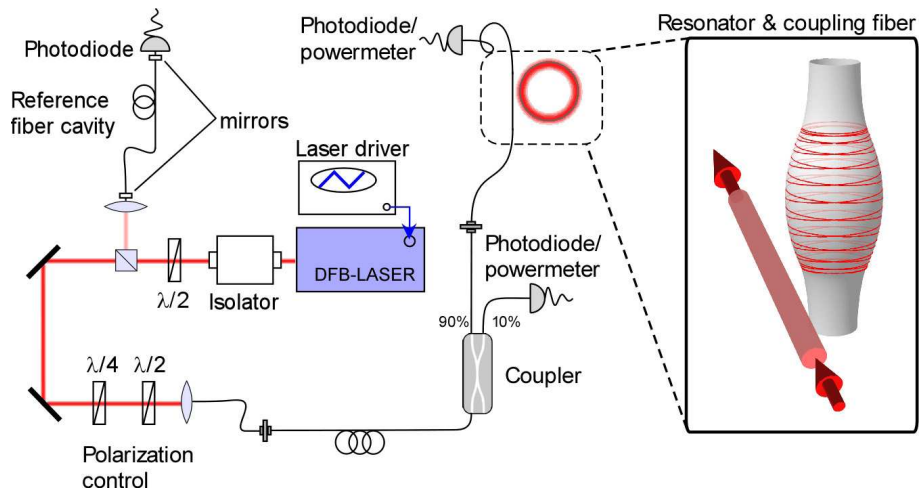


Figure 12: Schematic of the optical setup.

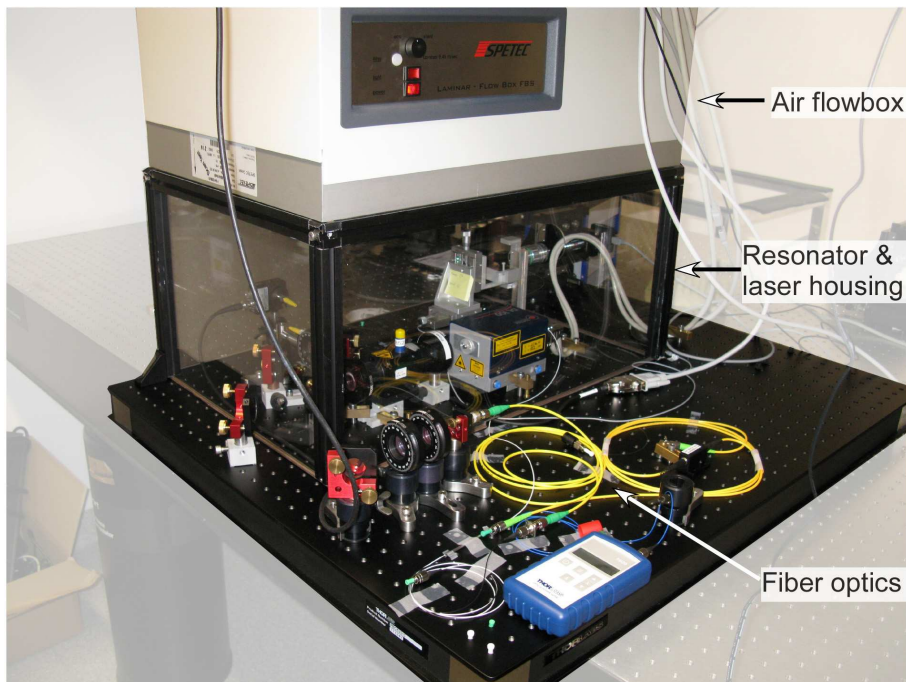


Figure 13: Picture of the experimental setup showing (1) the laser and resonator coupling setup housed in a air flowbox, and (2) the optical components.



Figure 14: CLASS 3B LASERS ARE HAZARDOUS TO THE EYE FROM DIRECT BEAM VIEWING, AND FROM SPECULAR REFLECTIONS EVEN FOR SHORT AND UNINTENTIONAL EXPOSURES! THEREFORE IT IS ABSOLUTELY NECESSARY TO TAKE OVERALL SAFETY MEASURES WHEN OPERATING THE SOURCE.

## 4 Laser Safety

- Avoid any back-reflection into the aperture of the laser head. Permanent damage to the laser diode can occur.
- Never connect or disconnect the cable between the control unit and the laser source. These acts can lead to laser hazard for you and possible permanent damage to the laser diode.
- Never exceed the temperature or current limits set on the laser controller. Permanent damage to the laser diode can occur.

### 4.1 Handling Instructions

- Keep the room clean and wash your hands. Most of the optical components are very sensitive to dirt – don't touch the the optical surfaces.
- Remove rings, bracelets, watches, etc. . . from your hands when working with the experiment. This ensures that the laser light cannot be reflected.
- Do not open the enclosure with the laser and coupling fibers.
- Do not turn any screws of the kinetic mounts unless you know what your doing. The alignment of the entire setup can easily be lost.
- Do not remove any of the parts from the breadboard. This may destroy the alignment of the setup.
- Handle the equipment with care, do not use any force.
- Turn off the laser when changing the connection of the fiber connectors between the power-meter and photodiode.
- Viewing the laser beam should not be necessary.
- The warning LEDs for the laser temperature and current controllers should never appear red.



- When evanescently coupling to the resonator, ensure there are no sources of vibration that might ruin the coupling: e.g., only touch the setup very carefully, do not close the door suddenly, turn off the air flowbox, be extra careful not to hit the table or any neighboring furniture.

## 5 Experimental Procedure

The experiment involves taking several different measurements, which are outlined in the subsections below:

1. **Excitation of a WGM:** The first task is to couple light into the resonator using the coupling fiber in order to excite a WGM. Observe the WGM with a microscope and CMOS camera.
2. **Evanescent coupling:** Once you know how to align the coupling fiber with the resonator you will again excite the WGM, but this time with an air gap between the coupling fiber and resonator. The importance of polarization on the mode spectrum of the resonator will be emphasized.
3. **Study evanescent coupling and resonator properties with controllable resonator–fiber gap:** Next, you will slowly and carefully move the coupling fiber towards the resonator while observing a mode on the oscilloscope. Starting in the very under-coupled regime (see sec. 2.1) and ending in the very over-coupled regime, the resonator loss-rate can be controlled. From the recorded data it is possible to determine the losses at the resonator–fiber coupling point.

### 5.1 Startup

Before starting, ensure that you are familiar with setup and know the function of each piece of equipment.

1. **Computer:** Open the camera software (uc480 Viewer) and stepper motor software (PIMikroMove), see Fig. 15. *Never close PIMikroMove because the stepper motor will need to re-align once restarted.* Set the camera exposure time to several seconds and record an image of the resonator.
2. **Laser and coupling fiber:** Turn on the laser and measure the power in the fiber at the 10% output of the fiber coupler using the power-meter (see Fig. 12 and Fig. 16). Also measure the power transmitted past the coupling fiber after. Determine the transmission efficiency of the coupling fiber. Notes: 1) there is a fiber adapter connecting the 90% output of 10/90 fiber coupler to the input of the coupling fiber, which has an efficiency of 70%. 2) The resonator should NOT touch the coupling fiber during the measurement. 3) The scan module of the laser controller should be turned off (see Fig. 17). 4) Contact the instructor if you measure less than 50% transmission efficiency.

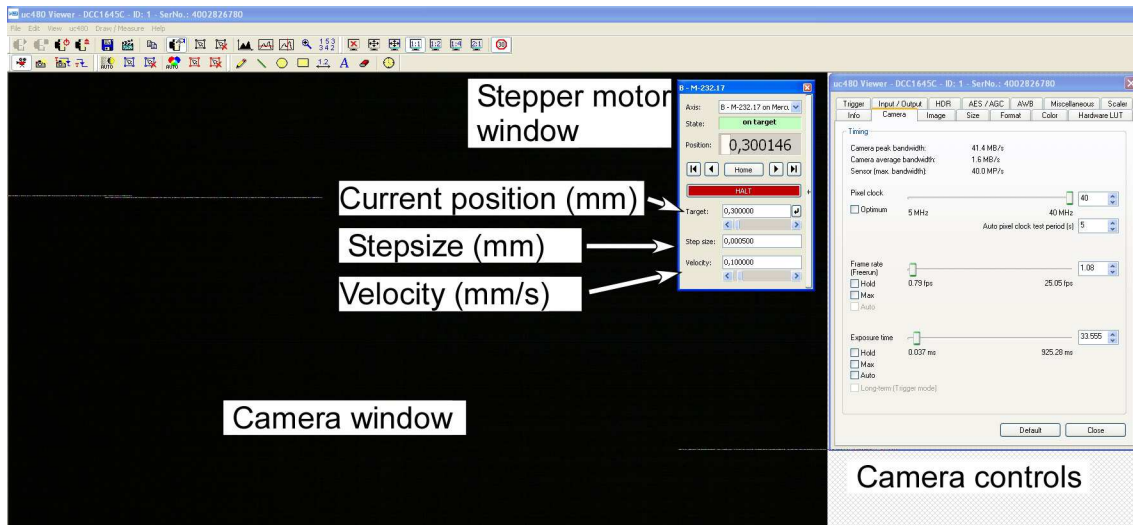


Figure 15: Software for operating the CMOS camera (uc480 Viewer) and moving the coupling fiber using the stepper motor (PIMikroMove).

3. **Oscilloscope:** Turn on the oscilloscope and connect a USB stick to the port. Data from the oscilloscope should be saved onto the USB stick. Note: save the CSV files, not just screen-shot pictures. See Fig.18.
4. **Piezo controller:** Turn on the controller and turn the voltage to the maximum value of 60 V (see Fig. 19). Reducing the voltage corresponds to moving the coupling fiber towards the resonator.

## 5.2 Excitation of a WGM

1. **Laser:** Set the current to 45 mA. **Warning: This current corresponds to several mW of optical power, which is harmful if accidentally viewed. Use the provided laser goggles.**
2. **Detectors:** Monitor and record the power in the fiber by connecting the 10% output of the 10/90 coupler to the power-meter. Attach the output of the coupling fiber to a 25 dB attenuator and connect this to the photodiode.
3. **Camera:** Run the camera and set the frame-rate to around 10–15 frames per second and increase the exposure time to the maximum allowable value for this frame-rate setting.
4. **Flowbox:** Since evanescent coupling is *very* sensitive to any vibrations, turn off the flow box and take note of the cautions in Sec. 4.1.
5. **Alignment of coupling fiber:** Set the step size to 0.005 mm and the velocity to 0.005 mm/s. The target position should be around 0.3 mm. Slowly approach the resonator by decreasing the target position until the fibers are in contact; use the arrow buttons. Hint: At around 0.05–0.2 mm the coupling fiber should be in contact with the resonator. This will be obvious because the resonator will start fluorescing green and appear bright on the camera picture. Notes: (1) some modes will appear more green than others and some

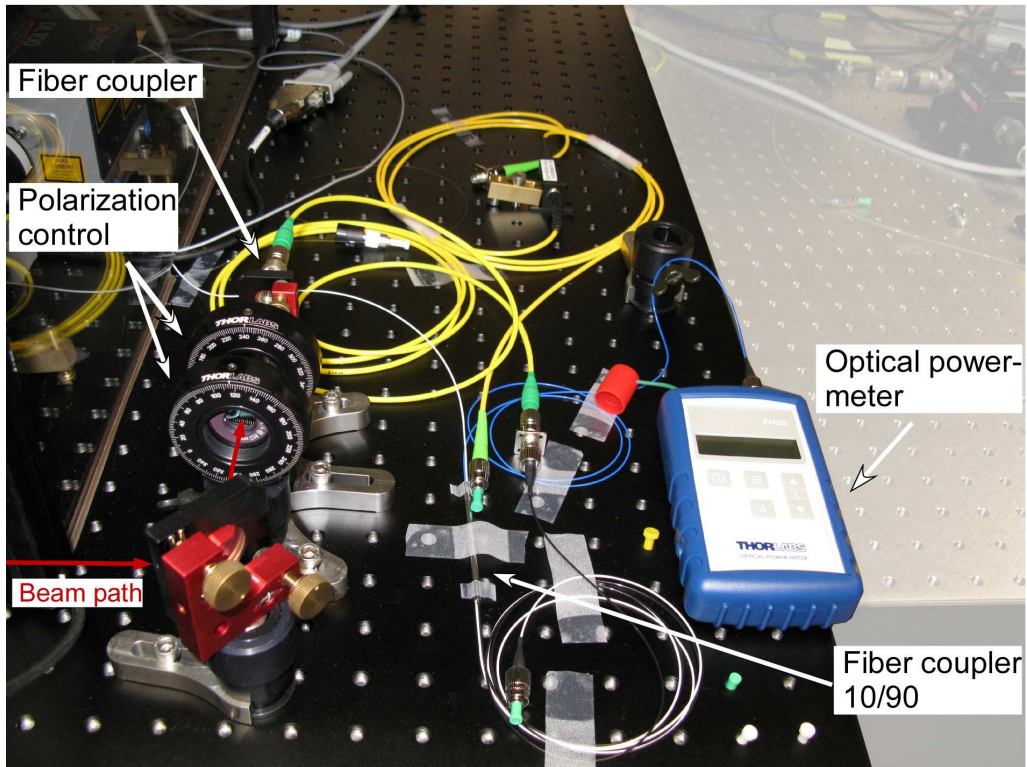


Figure 16: Setup of the optical and measurement components.

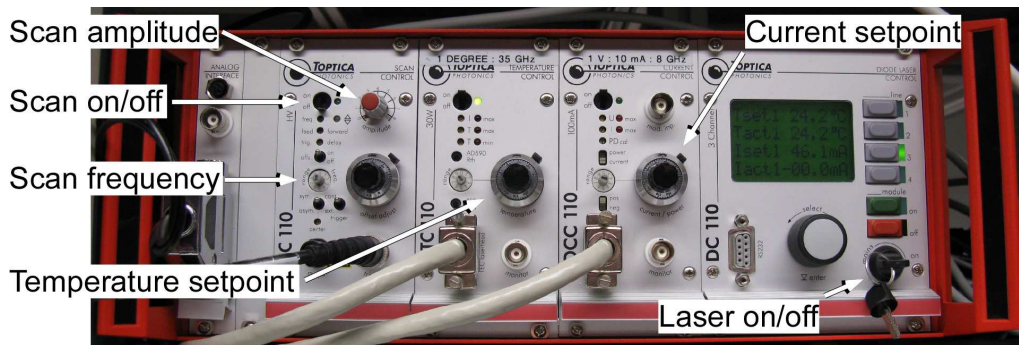


Figure 17: The laser controller (Left-to-right): 1) Scan module: scan the laser frequency when performing spectroscopy of the resonator modes, 2) Temperature controller: control the temperature of the DFB laser diode. This can be varied and causes the frequency of the laser to shift. 3) Current controller: controls the current going to the laser diode. Increasing current  $\equiv$  increasing optical power.

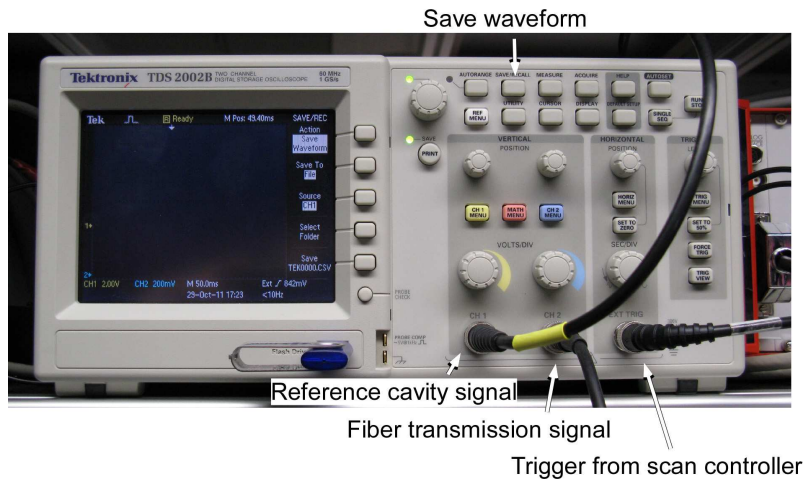


Figure 18: The oscilloscope is used to record the transmission of the coupling fiber and 1 m reference cavity when scanning the laser frequency with the laser scan module. The oscilloscope is synchronized with the scan module through the trigger channel.

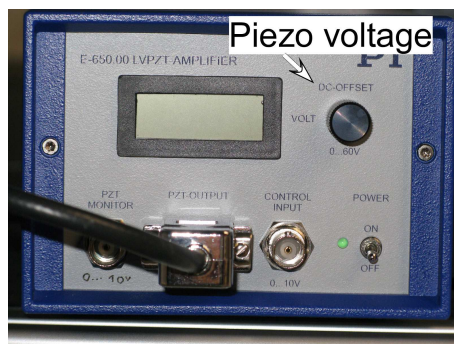


Figure 19: The piezo driver controls the fine positioning of the coupling fiber.

modes will just show a bright white blurry mode structure. (2) The laser light appears white on the camera picture.

- (a) Record the target position on the PIMikroMove where the coupling fiber came into contact.
- (b) Manually change the laser frequency until you find a green fluorescing mode. Hint: scan the temperature of the laser. Take a picture of the mode.
- (c) Turn on the laser scan module and set the amplitude to the 0-setting — this scans the laser frequency. Your mode will disappear. Find new modes.
- (d) Observe the resonance peaks of the reference cavity on the oscilloscope and adjust the settings (i.e., voltage scale and time scale) as necessary. Note: the scan module unfortunately causes the laser power to vary with laser frequency.
- (e) Reduce the scan amplitude and very slowly adjust the temperature setpoint of the laser so that you "zoom" into a mode or a group of 2–3 modes. Preferably choose a mode that fluoresces green. Demonstrate this last step to your instructor.

### 5.3 Evanescent Coupling with an air gap

As mentioned in Sec. 5, the next goal is to evanescently couple light to the resonator mode while maintaining an air gap. Success in this experiment will involve mastering this delicate procedure!

1. **Laser:** Set the current to around 20–25 mA so that the transmission signal from photodiode has an amplitude of 0.5–5 V. Record the power at the power-meter to calculate how much power is at the resonator. If it is more than 40  $\mu\text{W}$ , then reduce the current further. Note: the photodiode signal saturates at around 10 V. Turn on the laser scan module and set the amplitude to the 0-setting — this scans the laser frequency.
2. **Alignment:** Pull the fiber away from the resonator. Due to van der Waals and electrostatic effects, the fibers tend to stick together. Set the step size to 0.2 mm and the speed to 0.1 mm/s and move the fiber back in one step. The travel range of the piezo is only 18  $\mu\text{m}$ , so you need to get the coupling fiber to within 18  $\mu\text{m}$  distance of the surface using the stepper motor. Only then can you use the piezo.
  - (a) **Stepper-motor:** Now, move forward again by setting the target position to the position you recorded in Sec. 5.2 where the fibers made contact minus 30  $\mu\text{m}$ . If the fibers immediately stick again, press the move backward button and move forward again by setting the target position to the position where the fibers made contact minus 50  $\mu\text{m}$ . If necessary, record the new target position of the PIMikroMove where the coupling fiber makes contact with the resonator.
  - (b) **Piezo:** You can now use the piezo. Slowly turn the offset knob (e.g. 1 turn per 10 seconds) of the piezo driver and look for the sudden appearance dips in the transmission spectrum. Stop when you see these dips. These dips are of course WGM modes. Reduce the amplitude of the scan module so that the laser scans a range of around 2–5 GHz. Hint: use the reference cavity. If necessary, very slowly change the frequency offset of the laser until you find a mode. Hint: change the temperature

setpoint. Adjust the piezo until the mode dip is about 10–30%. Hint: it is sometimes easier to work with a mode with low  $Q$ -factor.

- (c) **Polarization:** What happens to the mode when you rotate the polarization of the light? Maximize the size of the dip by turning the waveplates. This is an iterative process and is very important for the measurements in the next section.
- (d) **Troubleshooting:** If the fibers come into contact, you will see a sudden change in the shape of the mode spectrum, the mode may become broader, and the resonator image may become brighter. However, the best way to know if they are in contact is to check if it is possible to make the WGM mode disappear by pulling back the fiber with the piezo. If in contact, then go back to the start of step 2 (if you have found a mode already, then leave the scan amplitude at 200–500 MHz).

#### 5.4 Evanescent Coupling and Resonator Properties as a function of Resonator–Fiber Gap

The aim of this part of the experiment is to experimentally investigate the properties of the resonator coupling fiber and then to compare these measurements with the above theoretical results. This section is the most important in terms of recording data.

**Mode spectra vs distance:** The task is to record the spectra of the mode you used in Sec. 5.3 for different resonator–fiber gaps. Record (1) spectra onto a USB-stick, and (2) the corresponding piezo voltages. Do not change the polarization during these measurements. Show the measurements to the instructor once finished.

1. Start in the very **under-coupled regime** where the mode dip is around 1% and only very slightly visible. Increment the piezo voltage in steps of 0.2 V and record the spectrum after each step. Improve the noise statistics by recording three spectra for each step.
2. As the distance gets smaller, the transmission at the center of the mode will be at its minimum value, i.e., the **critically-coupled regime**. When optimally aligned, it may be possible to get the dip down to less than 10% transmission.
3. For even smaller distances the transmission begins to increase again, i.e., the **over-coupled regime**. Measurements in this regime are very sensitive to vibration. Eventually, the fibers will come into contact and you must try to decide if the fibers touched because of a vibration spike or not. If you can take several measurements in the over-coupled regime and the transmission increases to >70%, then vibration is probably not a big problem.
4. **Troubleshooting:** What if the fibers touch? It may not be necessary to re-do the whole measurement if you can re-align the fiber so that the size of the resonance dip is the same as before the fibers touched. Note that the piezo voltage at this position will probably not be the same as before the fibers touched. This is ok, but you need to correct for this in your data analysis. You can then continue with the measurements.

Show the raw data to your instructor when finished.

Once all measurements are finished, turn off the equipment and turn on the flowbox.

### **End-of-experiment Check-list**

- **Coupling fiber:** Pull back the fiber so that it is not touching the resonator. Target position: 0.3 mm.
- **Laser:** Turn off the laser and scan module. Do NOT turn off the temperature or current controllers.
- **Others:** Turn off the oscilloscope, photodiode, camera software, piezo controller (turn to 0 V first).
- **Stepper-motor software:** Never turn this off.
- **Flowbox:** Turn *ON* the flowbox.

## 6 Analysis

Data analysis and understanding the measurements is a critical part of this experiment. The following is a guide to analyzing the data and builds on the introduction in Sec. 1.1. The data you record will be significantly different to the example data shown here. To do the analysis, you should use your favorite data processing program, e.g., *Origin* or also Matlab, Mathematica ... The laptop used in the experiment has Origin installed and it is suggested that you do all data analysis using this.

### 6.1 Resonator Properties

- **Critical coupling:** From the data in Sec. 5.4, find the spectrum where the transmission came closest to zero. Plot the mode spectrum: X-axis: units of frequency (MHz), Y-axis: relative transmission (0—1). State what power full transmission corresponds to. Fit an inverted Lorentzian curve to the data (In Origin, highlight the data and press Ctrl-Y to get the fitting options for function *Inverted\_Lorentz*). Hint: use the reference cavity to calibrate the time axis of the raw data from the oscilloscope. Be able to fit this curve before ending the experiment and contact your instructor if necessary. You probably will need to do this fitting step for all spectra.
  - Determine the (a) linewidth, (b) loaded quality factor, (c) intrinsic quality factor, and (d) photon lifetime at critical coupling. Include error estimates with  $\pm 1$  standard deviation. Hint: linewidth is a free parameter in the fitting function *Inverted\_Lorentz*.
  - Estimate the FSR assuming the diameter of the resonator is  $60 \mu\text{m}$ . Notes: the FSR is defined by one revolution of the light in a single ring around the resonator. Determine the finesse. Does finesse depend on under-over-critical-coupling? Why?
- **Resonant transmission vs coupling gap:** From the data in Sec. 5.4, study how the transmission changes with coupling gap. As an example, Fig. 20 shows the resonant transmission (at 0 MHz),  $T_{\text{res}}$ , for various values of  $x$  ranging from  $1.3 \mu\text{m}$  to the point at which the coupling fiber touches the resonator due to vibrations. Use the conversion  $\Delta x = \Delta U_{\text{piezo}} \cdot 0.25 \mu\text{m/V}$ . From this measurement a maximum value of  $T_{\text{res}} = 0.96$  is obtained in the over-coupled regime. Hint: For the x-axis, assume the  $0 \mu\text{m}$  position is the position where the fibers came into contact.
- **Quality factor vs coupling gap:** Determine the quality factor of the mode for each coupling gap. Plot the results ( $Q$  vs  $x$ ) and describe them.

Discuss sources of error, both random and systematic, and how they affect the measurements. Include error estimates and error bars where necessary (e.g. error in transmission,  $T_{\text{res}}$ , error in estimating the coupling gap,  $x$ , etc.). Indicate the three different coupling regimes in the plots.



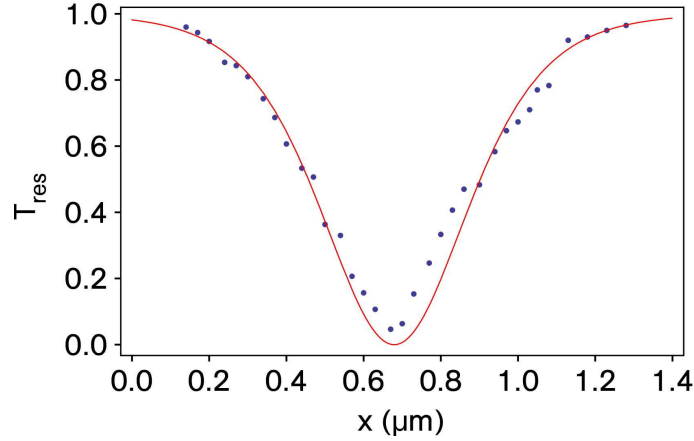


Figure 20: Transmission on resonance  $T_{\text{res}}$  for various values of the width  $x$  of the coupling gap. Critical coupling is achieved for  $x = 680$  nm. The data shows close agreement with the theoretical prediction from the model. The procedure for fitting the solid red line is explained in Sec. 6.2.

## 6.2 Losses introduced by the Ultra-Thin Coupling Fiber

The coupling fiber causes losses in the resonator. You can think of the coupling fiber as just another way of causing light to leave (and enter) the resonator, which obviously reduces the  $Q$ -factor. In this section, you will estimate the losses introduced by the coupling fiber when positioned near the bottle microresonator.

You have hopefully shown above that it is possible to recover almost 70–100% transmission in the over-coupled regime. The light detected at the photodiode in this case is completely transferred to the resonator and back to the coupling fiber. This means that the coupling between the resonator mode and the coupling fiber mode is much stronger than the intrinsic resonator losses. Intrinsic losses are, e.g., scattering of light from surface roughness or absorption by erbium ions causing green fluorescence.

Let us introduce the “coupling rate”  $\kappa_{\text{fiber}} = \tau_{\text{fiber}}^{-1}$  which describes the coupling between the coupling fiber mode and the resonator mode, the “rate of coupling to intrinsic loss channels”  $\kappa_0 = \tau_0^{-1}$  and the “rate of coupling to parasitic loss channels”  $\kappa_{\text{para}} = \tau_{\text{para}}^{-1}$ . The physical origin of  $\kappa_{\text{para}}$  is, e.g., scattering at the resonator–fiber coupling point. See Fig. 21 (b).

In the absence of a driving field, the power coupled from the resonator mode to a particular loss channel, having a decay time  $\tau$ , is proportional to  $\tau^{-1}$ . It is also useful to introduce the coupling parameter  $K$ . It is defined by the ratio of coupling between the coupling fiber mode and the bottle mode compared to the coupling to all other loss channels

$$K(x) = \frac{\kappa_{\text{fiber}}(x)}{\kappa_{\text{para}}(x) + \kappa_0}. \quad (20)$$

The transmission on resonance through the coupling fiber can be expressed by the coupling parameter

$$T_{\text{res}}(x) = \left( \frac{1 - K}{1 + K} \right)^2. \quad (21)$$

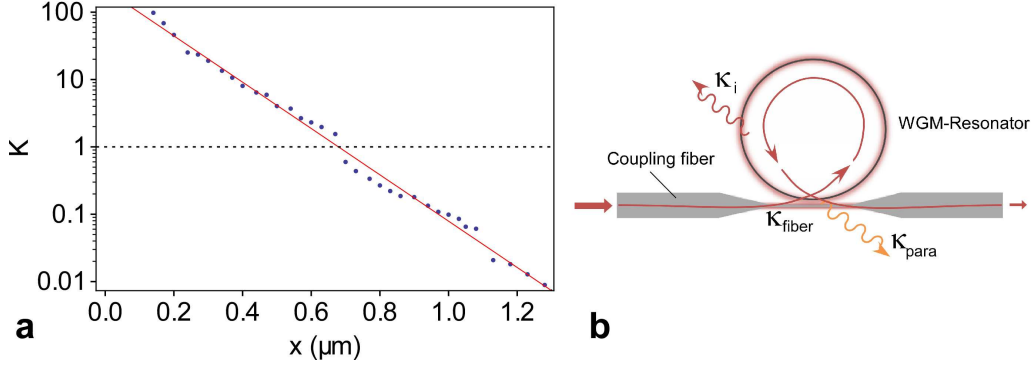


Figure 21: (a) Spatial variation of the coupling parameter calculated from  $T_{\text{res}}$ . The solid line (red) is a fit of the form  $K_0 \cdot \exp(-x/\gamma_0)$  with  $\gamma_0 = 130$  nm, which is the decay length of the evanescent field away from the resonator. A maximum value of  $K = 98$  is obtained close to the resonator surface. The horizontal dashed line indicates the critical coupling point for which  $K = 1$ . (b) Schematic describing three coupling rates,  $\kappa_{\text{para}}$ ,  $\kappa_i$ , and  $\kappa_{\text{fiber}}$ .

In the presence of parasitic losses, the critical coupling point ( $K = 1$ ) is shifted towards the resonator surface, where  $\tau_{\text{fiber}}^{-1} = \tau_0^{-1} + \tau_{\text{para}}^{-1}$  is fulfilled. By inverting Eq. (21) it is possible to calculate the coupling parameter from  $T_{\text{res}}$ .

$$K = \left( \frac{1 \pm \sqrt{T_{\text{res}}}}{1 \mp \sqrt{T_{\text{res}}}} \right), \quad (22)$$

where the upper signs apply for transmissions in the over-coupled regime, whereas the lower signs apply for transmission values from the under-coupled regime. By defining

$$K^{-1} = K_I^{-1} + K_P^{-1}, \quad (23)$$

the coupling parameter can be split into an intrinsic part  $K_I = \kappa_{\text{fiber}}/\kappa_0$  and a parasitic part  $K_P = \kappa_{\text{fiber}}/\kappa_{\text{para}}$ . The so-called “ideality”  $I$  quantifies the parasitic losses with respect to the coupling rate  $\kappa_{\text{fiber}}$ ,

$$I(x) = \frac{\kappa_{\text{fiber}}(x)}{\kappa_{\text{para}}(x) + \kappa_{\text{fiber}}(x)} = \frac{1}{1 + K_P^{-1}}. \quad (24)$$

For  $I = 1$  the ultra-thin fiber coupler introduces no parasitic losses. As an example, Fig. 21 (a) shows the variation of  $K$  with the width  $x$  of the coupling gap, calculated from the measurement presented in Fig. 20 using Eq. (22). For a decreasing gap the fiber coupling  $\kappa_{\text{fiber}}$  increases. Following Eq. (23) we see that therefor the influence of  $K_I$  on the coupling parameter  $K$  is reduced so that for very small gaps the parasitic losses can dominate the coupling. In this case one would observe a saturation of  $K$  toward  $K_P$  when the coupling fiber approaches the resonator. In Fig. 21 (a) we find that, as expected from the single mode properties of the ultra-thin fiber coupler,  $\log(K)$  shows no deviation from the linear behavior. To estimate a lower boundary for  $I$  here, we can use the maximal value of  $K = 98$  in the strongly over-coupled regime instead of  $K_P$ , resulting in an ideality of  $I \geq 0.99$ .

**Coupling parameter,  $K$ , vs coupling gap,  $x$ :** From the data in Sec. 5.4, calculate the coupling parameter,  $\log(K(x))$ , for each coupling gap,  $x$ , and plot it. Note: We take the logarithm of  $K(x)$

because the evanescent field decays exponentially with distance from the fiber. Fit a line to the data and record the fitting errors (see Fig. 21). Using this line fitting equation, go back to Sec. 6.1 and fit a line to the data as in Fig. 20. The error in  $K$  depends on the error in resonant transmission,  $T_{\text{res}}$ . From Eq. 22 we find the standard deviation is

$$\frac{\sigma_K}{K} = \frac{\sigma_T}{\sqrt{2}T_{\text{res}}}, \quad (25)$$

where  $\sigma$  is the error. For  $\sigma_T$  this is the standard deviation from the three spectra you recorded for each coupling gap.

- Determine the *ideality* (see Eq. 24) from a data point in the deeply over-coupled regime (i.e. largest  $K$ ). Explain why  $K = 1$  at critical coupling.
- Interpret what is meant by a large *ideality*? What does it say about losses at the point where light evanescently couples between the coupling fiber and resonator?

**Photon coupling efficiency:** Finally, let's calculate the probability that a photon in the resonator is coupled into the coupling fiber. This is an important value to know in many applications where the loss of even single photons is an issue, e.g. in quantum information applications. The resonator photon could be lost by (1) absorbing erbium ions, (2) scattered out of the resonator because of surface roughness (i.e. intrinsic loss), (3) or scattered away by the coupling fiber (i.e. parasitic loss), or it can couple into the fiber.

The overall loss rate of the light stored inside the resonator  $\kappa_{\text{para}} + \kappa_0$  compared to the coupling rate  $\kappa_{\text{fiber}}$  is quantified using

$$E_{\text{photon}}(x) = \frac{\kappa_{\text{fiber}}(x)}{\kappa_{\text{para}}(x) + \kappa_0 + \kappa_{\text{fiber}}(x)} = \frac{1}{1 + K^{-1}} \quad (26)$$

This quantity describes the probability that a photon stored in the resonator is coupled back into fiber rather than being dissipated by intrinsic or parasitic losses. Figure 22 shows a plot of  $E_{\text{photon}}$  as a function of the width  $x$  of the coupling gap.

From the data in Sec. 5.4, plot  $E_{\text{photon}}$  as a function of  $x$ . Fit a line as described in the caption for Fig. 22. Discuss the plot. What is the efficiency in the very over/critically/coupled-coupled regimes? What are the advantages/disadvantages of operating in the very over-coupled regime.

## 7 Writing the Report

The most important part of the report is the data analysis section. The quality of the results and the error analysis is also very important. An ideal report should consist of the following:

- **Abstract:** A very short summary of the main results and outcome. This section should be no more than 4 sentences maximum.
- Give a short **introduction** to (1) evanescent fields and how they arise, (2) the WGM bottle resonator and some main differences compared to a Fabry-Pérot resonator.

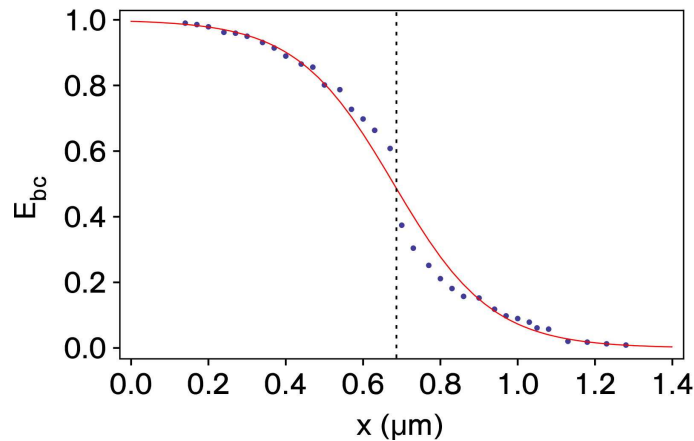


Figure 22: Dependency of  $E_{\text{photon}}$  on the width  $x$  of the coupling gap. The red line corresponds to the values obtained for  $K$  from the fit in Fig. 21.

- Briefly describe the **experimental setup**. Include your picture of the resonator. Describe how to measure (1) the transmission efficiency of the coupling fiber, and (2) how to calculate how much power is coupled into the resonator.
- **Data analysis:** include all your work (plots and analysis) from Sec. 6. Also include the things you measured in Sec. 6.1 and Sec. 5.3, e.g., transmission efficiency of the coupling fiber, affect of light polarization on the resonator modes, power of the laser beams,  $Q$ -factor of the resonator mode etc. Discuss sources of error.
- **Conclusion and summary:** briefly mention what you learned. What were the main results? Remember to give error estimates where necessary. Do you have any suggestions for improvements that might help other students doing this experiment? Was the theory too difficult/easy/just right? Were the measurements too difficult/easy/just right? Was the data analysis too difficult/easy/just right?
- **Appendix:** include all plots of the mode spectra.

## 8 Optional Exercises

Once you have finished reading the introductory sections, test your knowledge by answering these exercises. The exercises are optional but strongly recommended.

- P 1 **True or False:** An evanescent wave exists on the transmitted side of an interface.
- P 2 **Decay Length:** Light ( $\lambda = 852$  nm) reflects internally from a glass surface ( $n = 1.5$ ) surrounded by air. The incident angle is  $\theta_i = 45^\circ$ . An evanescent wave travels parallel to the surface on the air side. At what distance from the surface is the amplitude of the evanescent wave  $1/e$  of its value at the surface?
- P 3 Derive a relationship between quality factor,  $Q$ , and finesse,  $F$ .
- P 4 **Decay Distance:** A WGM resonator has a  $Q$  of  $1 \times 10^8$  at critical coupling. After what distance will a light pulse travel in a resonator mode before decaying to  $1/e$  of its energy.  $\lambda = 852$  nm,  $n = 1.5$ .
- P 5 **Optical Energy Decay Time:** How much time does it take for the optical energy stored in a Fabry P erot resonator of finesse  $F = 1 \times 10^6$ , length  $d = 1$  cm, and refractive index  $n = 1$ , to decay to one-half of its initial value? Assume there is no driving field, i.e., no light is being coupled into the resonator.
- P 6 **Spectral Response:** The transmission spectrum of a WGM resonator was measured with a tunable, monochromatic laser source at around 852 nm. Periodic dips in the transmission, corresponding to the fundamental resonator mode, are observed with a spacing of 2 THz. The FWHM of the dips are 10 MHz. What is the quality factor?
- P 7 **Quality Factors:** The quality factor at critical coupling is a factor of two smaller than when measured in the very under-coupled regime. Why?
- P 8 **Critical coupling:** When the position of the coupling fiber is carefully chosen and the polarization is correct, it is possible to get the resonance dip of the WGM down to 1% transmission. If there is little or no transmitted light at the center-frequency of the mode, then where does it go? Energy conservation is not violated.

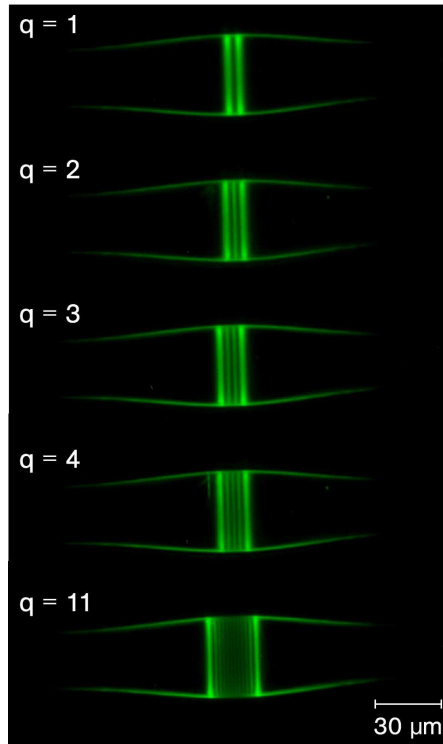


Figure 23: Experimental pictures of several different bottle modes observed via the up-converted green fluorescence of erbium ions doped in a bottle microresonator.

## A Appendices

### A.1 Emission of green fluorescence from bottle modes

When resonantly exciting bottle modes at a wavelength around 852 nm, the erbium ions emit fluorescence light at a wavelength around 540 nm in an two-photon up-conversion process. This green fluorescence is then observed using the optical microscope. It is of course possible to also make resonators that are not doped with erbium ions.

## References

- [Mes04] D. Meschede, *Optics, Light and Lasers* (Wiley-VCH, Weinheim, 2004).
- [Hau84] H.A. Haus, *Waves and Fields in optoelectronics* (Prentice-Hall, Englewood Cliffs, New Jersey, 1984).
- [Hec89] E. Hecht, *Optik* (Addison-Wesley, Bonn, 1989).
- [Vah03] For a nice overview: K.J. Vahala, *Optical microcavities*, *Nature* **424**, 839-846 (2003)  
(Find it here, for example: [http://www.reading.ac.uk/physicsnet/units/4/4phla/Papers/Nature03\\_OpticalMicrocavities\\_Vahala.pdf](http://www.reading.ac.uk/physicsnet/units/4/4phla/Papers/Nature03_OpticalMicrocavities_Vahala.pdf)).